



# Diacylglycerol kinase $\epsilon$ deficiency preserves glucose tolerance and modulates lipid metabolism in obese mice<sup>§</sup>

Louise Mannerås-Holm,\* Milena Schönke,\* Joseph T. Brozinick,<sup>†</sup> Laurène Vetterli,\* Hai-Hoang Bui,<sup>†</sup> Philip Sanders,<sup>†</sup> Emmani B. M. Nascimento,\* Marie Björnholm,\* Alexander V. Chibalin,\* and Juleen R. Zierath<sup>1,\*</sup>

Section of Integrative Physiology, Department of Molecular Medicine and Surgery and Department of Physiology and Pharmacology,\* Karolinska Institutet, Stockholm, Sweden; and Lilly Research Laboratories,<sup>†</sup> Eli Lilly and Company, Indianapolis, IN

**Abstract** Diacylglycerol kinases (DGKs) catalyze the phosphorylation and conversion of diacylglycerol (DAG) into phosphatidic acid. DGK isozymes have unique primary structures, expression patterns, subcellular localizations, regulatory mechanisms, and DAG preferences. DGK $\epsilon$  has a hydrophobic segment that promotes its attachment to membranes and shows substrate specificity for DAG with an arachidonoyl acyl chain in the sn-2 position of the substrate. We determined the role of DGK $\epsilon$  in the regulation of energy and glucose homeostasis in relation to diet-induced insulin resistance and obesity using DGK $\epsilon$ -KO and wild-type mice. Lipidomic analysis revealed elevated unsaturated and saturated DAG species in skeletal muscle of DGK $\epsilon$  KO mice, which was paradoxically associated with increased glucose tolerance. Although skeletal muscle insulin sensitivity was unaltered, whole-body respiratory exchange ratio was reduced, and abundance of mitochondrial markers was increased, indicating a greater reliance on fat oxidation and intracellular lipid metabolism in DGK $\epsilon$  KO mice. Thus, the increased intracellular lipids in skeletal muscle from DGK $\epsilon$  KO mice may undergo rapid turnover because of increased mitochondrial function and lipid oxidation, rather than storage, which in turn may preserve insulin sensitivity. In conclusion, DGK $\epsilon$  plays a role in glucose and energy homeostasis by modulating lipid metabolism in skeletal muscle.—Mannerås-Holm, L., M. Schönke, J. T. Brozinick, L. Vetterli, H-H. Bui, P. Sanders, E. B. M. Nascimento, M. Björnholm, A. V. Chibalin, and J. R. Zierath. **Diacylglycerol kinase  $\epsilon$  deficiency preserves glucose tolerance and modulates lipid metabolism in obese mice.** *J. Lipid Res.* 2017. 58: 907–915.

**Supplementary key words** lipid kinase • lipidomics • insulin resistance • muscle • animal models • obesity • diabetes

This research was supported by the Strategic Research Program in Diabetes at Karolinska Institutet, European Research Council Ideas Program (ICE-BERG, ERC-2008-AdG23285), Swedish Research Council (2011-3550), Swedish Diabetes Foundation (DIA2012-082), Swedish Foundation for Strategic Research (SRL10-0027), Diabetes Wellness Sweden, and Novo Nordisk Foundation.

Manuscript received 21 December 2016 and in revised form 13 February 2017.

Published, JLR Papers in Press, February 28, 2017

DOI <https://doi.org/10.1194/jlr.M074443>

Copyright © 2017 by the American Society for Biochemistry and Molecular Biology, Inc.

This article is available online at <http://www.jlr.org>

Type 2 diabetes is a heterogeneous metabolic disorder characterized by peripheral insulin resistance, impaired insulin secretion, and disturbed glucose and lipid metabolism (1, 2). Consequently, a multitude of intervention strategies are required in order to maintain normal glucose and energy homeostasis. Increased accumulation of lipid intermediates, such as triglycerides, diacylglycerol (DAG), ceramides, and long-chain fatty acid CoA, in liver and skeletal muscle can partly explain the development of insulin resistance (2). Therefore, elucidation of the cellular mechanisms that control intracellular lipid accumulation may give insight into the pathogenesis of type 2 diabetes. Lipids act as signaling molecules that modulate pathways controlling various metabolic functions (3). Thus, enzymes regulating lipid metabolism control the bulk flux of metabolites and the synthesis and degradation of key signaling molecules that may play a role in glucose and energy homeostasis.

Diacylglycerol kinases (DGKs) catalyze the phosphorylation and conversion of DAG into phosphatidic acid (PA) and thereby terminate DAG signaling (4, 5). Ten mammalian DGK isozymes have been classified into five subgroups on the basis of their primary structure (6). These DGK isozymes are unique, not only with respect to their primary structures, but also in expression pattern, subcellular localization, regulatory mechanisms, and DAG preferences. Previously, we revealed a crucial role for DGK $\delta$  in the regulation of glucose and energy homeostasis in type 2 diabetes (7). DGK $\delta$  protein deficiency impairs 5' adenosine

Abbreviations: CS, citrate synthase; DAG, diacylglycerol; DGK, diacylglycerol kinase; EDL, extensor digitorum longus; GK, glycerol kinase; HADH, hydroxyacyl-CoA dehydrogenase; HFD, high-fat diet; IPGTT, intraperitoneal glucose tolerance test; KHB, Krebs-Henseleit bicarbonate buffer; PA, phosphatidic acid; PC, phosphatidylcholine; PE, phosphatidylethanolamine; RER, respiratory exchange ratio; VO<sub>2</sub>, oxygen consumption.

<sup>1</sup>To whom correspondence should be addressed.

e-mail: [Juleen.zierath@ki.se](mailto:Juleen.zierath@ki.se)

<sup>§</sup>The online version of this article (available at <http://www.jlr.org>) contains a supplement.

monophosphate-activated protein kinase signaling, lipid metabolism, and skeletal muscle energetics (8). However, the direct role of other DGK isozymes in the development of metabolic disorders, including insulin resistance, obesity, or type 2 diabetes, is unknown.

Mammalian DGK $\epsilon$  is the smallest and, in terms of primary structure, simplest mammalian DGK identified to date, with several distinct structural features. DGK $\epsilon$  is the only isoform with a hydrophobic segment that promotes attachment of the protein to membranes (9). Moreover, DGK $\epsilon$  is the only DGK family member that shows substrate specificity for DAG with an arachidonoyl acyl chain in the *sn*-2 position of the substrate (10, 11). As such, the PA produced by DGK $\epsilon$  is enriched in polyunsaturated fatty acids, particularly arachidonate, suggesting that DGK $\epsilon$  may have a more prominent role than other DGK isozymes in enriching inositol phospholipids with unsaturated fatty acids (12). The DAG species preferentially targeted by DGK $\epsilon$  are abundant in insulin-resistant skeletal muscle (13). Thus, DGK $\epsilon$  may influence glucose or energy homeostasis by altering the intracellular lipid species and subsequent lipid-mediated signal transduction.

DGK $\epsilon$  is highly expressed in testis, brain, and spleen, with lower but comparable levels in skeletal muscle and adipose tissue (14). In brain, DGK $\epsilon$  modulates neuronal signaling pathways linked to synaptic activity, neuronal plasticity, and epileptogenesis (15). In spleen, DGK $\epsilon$  mRNA is upregulated in T cells in response to inflammatory stimuli (16), implicating a role in immunology (16). In the heart, DGK $\epsilon$  overexpression prevents cardiac hypertrophy (17). Recessive mutations in DGK $\epsilon$  causes atypical hemolytic-uremic syndrome, with associated hypertension, hematuria, and proteinuria, and chronic kidney disease (18). Although the role of DGK $\epsilon$  in metabolic disease is unknown, DGK $\epsilon$  mRNA is reduced in extensor digitorum longus (EDL) muscle and epididymal adipose tissue from *ob/ob* mice (19). Given this diverse physiology, we explored the role of DGK $\epsilon$  in the regulation of energy and glucose homeostasis in relation to diet-induced insulin resistance and obesity using DGK $\epsilon$  KO mice. Lipidomic analysis revealed elevated unsaturated and saturated DAG species in the skeletal muscle of DGK $\epsilon$  KO mice, which was paradoxically associated with increased glucose tolerance. Although skeletal muscle insulin sensitivity was unaltered in DGK $\epsilon$  KO mice, whole-body respiratory exchange ratio (RER) was reduced, indicating that fat oxidation was increased. Thus, DGK $\epsilon$  plays a role in both glucose and energy homeostasis.

## MATERIAL AND METHODS

### Genetically modified mice

Male whole-body DGK $\epsilon$  KO mice and WT littermates were used. The generation of DGK $\epsilon$  KO mice has previously been described (15). Mice were fed a normal standard rodent chow (Lantmännen, Stockholm, Sweden) until the end of the study or a high-fat diet (HFD; 55% fat by calories; TD.93075; Harlan Teklad, Horst, Netherlands) from 5 weeks of age until the end of

the study. Animals were housed in a temperature-controlled (22°C) facility with a 12 h light-dark cycle with free access to food and water. Body weight was monitored weekly. The experimental protocol was approved by the regional animal ethical committee (Stockholm, Sweden).

### Lipidomic analysis in skeletal muscle

Lipidomic analysis was performed in gastrocnemius muscle from 4 h fasted, HFD-fed DGK $\epsilon$  KO mice and WT mice 17–20 weeks of age. Chloroform (600  $\mu$ l) and methanol (240  $\mu$ l) were added to glass vials with aliquots of muscle homogenate. An internal standard was added, and the samples were disrupted on a Qia-gen TissueLyser for 2 min at 20 Hz. Thereafter, water (250  $\mu$ l) was added to break the phases, and the samples were shaken once again. The tubes were subjected to centrifugation for 5 min at 4,000 rpm. An 800  $\mu$ l aliquot of 1:1 isopropyl alcohol:methanol and 20 mM of ammonium acetate was added to 400  $\mu$ l of the bottom phase of the extraction. A Spark-Holland autosampler was used to administer 200  $\mu$ l into the infusion stream. Lipidomic analysis was performed by achieving a steady-state infusion of the chloroform/methanol extract of samples into an AB-Sciex 5600 QQ ToF mass spectrometer. The mass spectrometer was operated in electrospray mode at a flow rate of 20 ml/min. The sample was spiked with a series of lipid internal standards, and the data were normalized with these internal standards, resulting in a height ratio output. The internal standards used in the assay were C15:0 DAG, D5 Tripalmitin, C14:0 phosphatidylcholines (PCs), C17:0 sphingomyelin, C17:0 ceramide, C15:0 lysophosphatidylcholines, and C15:0 phosphatidyletanolamine (PE).

### Triglyceride content in liver

Triglyceride (TG) was extracted from liver tissue of mice 17–20 weeks of age using a heptane:isopropanol (3:2) mix. TG concentration was determined with a Trig/GB kit (Roche Diagnostics, Indianapolis, IN).

### Body weight and body composition

Body weight of the mice was recorded each week from 6 to 13 weeks of age. Body composition (lean and fat mass) was determined in conscious mice at 16 weeks of age with an EchoMRI-100 system (Echo Medical Systems, LLC, Houston, TX).

### Glucose tolerance

An intraperitoneal glucose tolerance test (IPGTT) was performed in DGK $\epsilon$  KO and WT mice (15–17 weeks of age). Glucose (2 mg/g of body weight) was administered to 4 h fasted mice by intraperitoneal injection. Blood samples were obtained via the tail vein before and 15, 30, 60, and 120 min after the glucose injection for measurement of glucose concentration (OneTouch Ultra Glucose Meter; Lifescan). Plasma insulin was analyzed in samples obtained before and 15 min after the glucose injection with an Ultra-Sensitive Mouse Insulin ELISA Kit (Crystal Chem, Downers Grove, IL).

### Whole-body energy homeostasis

Oxygen consumption ( $VO_2$ ), carbon dioxide output ( $VCO_2$ ), RER, energy expenditure, and locomotor activity were measured with a Comprehensive Laboratory Animal Monitoring System (Columbus Instruments, Columbus, OH). Mice (16–21 weeks of age) were housed individually in metabolic cages with ad libitum access to food and water. Mice were acclimatized to the metabolic cages for 48 h prior to a 24 h period of automated recordings every 20 min. Calorimetry was determined by an open-circuit Oxy-max. Sample air from individual cages was passed through sensors to determine  $O_2$  and  $CO_2$  content.  $VO_2$  was calculated as the

difference between the input oxygen flow and the output oxygen flow.  $\text{VO}_2$  and  $\text{VCO}_2$  values were used to calculate RER and energy expenditure (heat – kcal/h). Spontaneous locomotor (ambulatory) activity was measured by consecutive beam breaks in adjacent beams under the 24 h period.

### Glucose transport in isolated skeletal muscle

Glucose uptake was assessed in isolated skeletal muscle from 4 h fasted chow- or HFD-fed mice (17–20 weeks of age). Incubation medium was prepared from a stock solution of Krebs-Henseleit bicarbonate buffer (KHB) supplemented with 5 mM of HEPES and 0.1% BSA (RIA grade) and was continuously gassed with 95%  $\text{O}_2$ /5%  $\text{CO}_2$ . Mice were anesthetized (2.5% avertin; 0.02 ml/g body weight), and the EDL and soleus muscles were removed. Muscles were incubated in the absence or presence of insulin (0.36 nM) at 30°C for 30 min in KHB containing 5 mM glucose and 15 mM mannitol and subsequently for 10 min in KHB containing 20 mM mannitol. Thereafter, 2-deoxy-glucose uptake was assessed in EDL and soleus muscles as described (7).

### Protein extraction and protein abundance measurement

Gastrocnemius muscles were homogenized in ice-cold homogenization buffer [20 mM Tris, pH 7.8, 137 mM NaCl, 2.7 mM KCl, 1 mM  $\text{MgCl}_2$ , 0.5 mM  $\text{Na}_3\text{VO}_4$ , 1% Triton X-100, 10% glycerol, 10 mM NaF, 0.2 mM PMSF, 1 mM EDTA, 5 mM  $\text{Na}_4\text{P}_2\text{O}_7$ , 1% [v/v] Protease Inhibitor Cocktail (Calbiochem, Darmstadt, Germany)] by using a mortar and pestle and TissueLyser II (Qiagen, Hamburg, Germany). Muscle lysates were subsequently rotated for 1 h at 4°C and subjected to centrifugation at 12,000 *g* for 10 min at 4°C. The supernatant was then collected, and the protein concentration was determined using a bicinchoninic acid protein assay kit (Pierce, Rockford, IL). Protein lysates were subsequently diluted with Laemmli buffer and heated for 20 min at 56°C. Equal amounts of protein were separated on precast Criterion XT Bis-Tris SDS-PAGE gradient gels (Bio-Rad, Hercules, CA) and transferred to PVDF membranes (Immobilion, Merck Millipore, Billerica, MA). Membranes were blocked in 7.5% milk in TBS-T for 1 h at room temperature and incubated overnight with a primary antibody at 4°C. Membranes were washed and incubated with the appropriate horseradish peroxidase-conjugated secondary antibody (Bio-Rad) in 5% milk for 1 h at room temperature. Proteins were visualized using enhanced chemiluminescence Western blot detection reagents from GE Healthcare (Waukesha, WI). Optical density of the bands was quantified by using Quantity One imaging system (Bio-Rad). Antibodies against citrate synthetase (ab96600), 3-hydroxyacyl-CoA dehydrogenase (ab154088), and glycerol kinase (ab 180525) were from Abcam (Nordic Biosite, Sweden). Equal loading of protein on the gels was ensured using Ponceau staining.

### Statistical analysis

Data are presented as means  $\pm$  SEM. Differences between genotypes were determined by unpaired two-tailed Student *t* test or two-way ANOVA, where applicable.  $P < 0.05$  was considered significant.

## RESULTS

### Impact of DGK $\epsilon$ on lipidomic profiles in skeletal muscle and lipid content in liver

To investigate the role of DGK $\epsilon$  in lipid metabolism, we assessed the intracellular lipid species in skeletal muscle and accumulation of TG in liver. Given that DGK $\epsilon$  is lowly expressed in liver (19), we restricted the lipidomic analysis to a survey of skeletal muscle. Lipidomic analyses were performed

in gastrocnemius muscle from HFD-fed DGK $\epsilon$  KO mice and WT mice using high-resolution LC/MS. The lipidomic analysis retrieved most of the major lipid classes, including DAGs (Fig. 1A, B), ceramides, cholesterol esters, lysophosphatidylcholines, PCs, PEs, phosphatidylserines, sphingomyelins, and TGs (supplemental Tables S1–S9). Strikingly, unsaturated (Fig. 1A) and saturated (Fig. 1B) DAG species were elevated in gastrocnemius muscle from HFD-fed DGK $\epsilon$  KO mice. This result suggests that DGK $\epsilon$  influences the balance of DAG species implicated in the development of peripheral insulin resistance. Malonyl-CoA and acetyl-CoA levels were unchanged between WT and KO mice ( $0.86 \pm 0.06$  vs.  $0.79 \pm 0.12$  nmol/g and  $1.76 \pm 0.22$  vs.  $1.80 \pm 0.19$  nmol/g, respectively). Total TG content was unchanged; however, short-acyl-chain TG species were elevated ( $P = .026$ ) in gastrocnemius muscle from HFD-fed DGK $\epsilon$  KO versus WT mice. To gain insight into the role of DGK $\epsilon$  in lipid metabolism in liver, we assessed hepatic TG content in 4 h fasted mice fed HFD or chow. Hepatic TG content was similar between DGK $\epsilon$  KO mice and WT mice, irrespective of diet (Fig. 1C). HFD promotes hepatic lipid accumulation to a similar extent in DGK $\epsilon$  KO mice and WT mice.

### DGK $\epsilon$ is dispensable for growth and maintenance of normal body composition

We next determined whether DGK $\epsilon$  is involved in the regulation of body weight and body composition. Body weight and growth curves were similar between DGK $\epsilon$  KO mice and WT mice fed either chow or HFD (Fig. 2A). Body composition was determined in 16-week-old mice by EchoMRI. Whole-body fat mass (Fig. 2B) and lean mass (Fig. 2C) were similar between DGK $\epsilon$  KO mice and WT mice fed either HFD or chow. Despite changes in skeletal muscle DAG content, DGK $\epsilon$  does not affect growth patterns or body composition.

### DGK $\epsilon$ deficiency enhances glucose homeostasis

Several lines of evidence implicate DAG accumulation in the development of insulin resistance (2, 20). Given the elevation in skeletal muscle DAG content in DGK $\epsilon$  KO mice, we next assessed glucose homeostasis. Paradoxically, glucose tolerance was improved in HFD-fed DGK $\epsilon$  KO mice as evidenced by a reduction in the blood glucose concentration 15 min following glucose administration and the decreased glucose area under the curve (AUC) in comparison with HFD-fed WT mice (Fig. 3A, B). Insulin levels in the fasting state, as well as during the IPGTT, were similar between HFD-fed DGK $\epsilon$  KO mice and WT mice (Fig. 3C), suggesting improved insulin sensitivity. The improvement in glucose tolerance was unexpected, given that earlier evidence implicating diacylglycerol accumulation contributes to the development of insulin resistance (2, 20). In contrast, glucose tolerance, fasting blood glucose, and plasma insulin levels were unaltered between chow-fed DGK $\epsilon$  KO mice and chow-fed WT mice (Fig. 3A, B, D).

### DGK $\epsilon$ deficiency does not alter glucose transport in skeletal muscle

To determine whether DGK $\epsilon$  directly modifies glucose metabolism in skeletal muscle, we assessed basal and



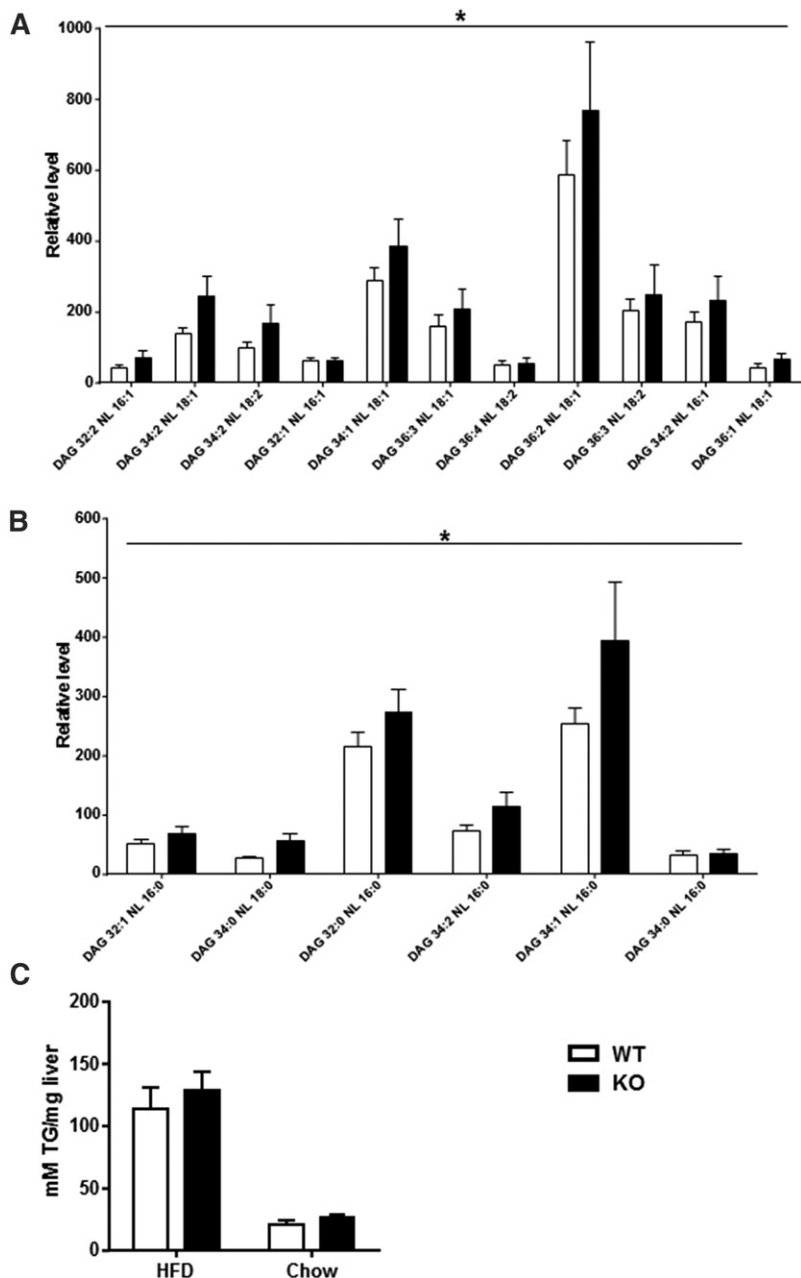


**Fig. 1.** Impact of DGK $\epsilon$  on DAG levels in skeletal muscle and lipid content in liver. Gastrocnemius muscle was obtained from HFD-fed DGK $\epsilon$  KO mice (solid bars) and WT mice (open bars) for analysis of unsaturated (A) and saturated (B) DAG species. The liver was obtained from HFD- or chow-fed DGK $\epsilon$  KO mice (solid bars) and WT mice (open bars) for biochemical assessment of total TG content (C). Results are presented as the mean  $\pm$  SEM for  $n = 5-9$  mice. \* $P < 0.01$  versus WT mice (genotype effect by means of two-way ANOVA).

insulin-stimulated glucose transport in isolated EDL and soleus muscle from 17- to 20-week-old DGK $\epsilon$  KO mice and WT mice fed either HFD or chow. Irrespective of diet, basal and submaximal insulin-stimulated 2-deoxyglucose transport in isolated EDL (Fig. 4A, C) and soleus muscle (Fig. 4B, D) were unaltered between DGK $\epsilon$  KO mice and WT mice.

#### DGK $\epsilon$ deficiency alters energy homeostasis by increasing whole-body lipid oxidation

Whole-body energy homeostasis was determined by indirect calorimetry (Fig. 5). The diurnal shifts in  $VO_2$  were similar between HFD-fed KO mice and WT mice (Fig. 5A). However, RER was reduced in HFD-fed DGK $\epsilon$  KO mice during both light and dark cycles, indicating increased whole-body lipid oxidation (Fig. 5B). Energy expenditure (Fig. 5C) was slightly reduced in HFD-fed DGK $\epsilon$  KO mice ( $P = .10$ )

during both light and dark cycles. Although we observed diurnal shifts in locomotor activity, general motor activity, as tracked by invisible infrared beams, was similar between HFD-fed DGK $\epsilon$  KO mice and WT mice (Fig. 5D). The reduced RER in HFD-fed DGK $\epsilon$  KO mice cannot be explained by decreased locomotor activity. Whole-body energy homeostasis ( $VO_2$ /RER/energy expenditure) and locomotor activity during both light and dark cycles were similar between chow-fed DGK $\epsilon$  KO mice and WT mice (Fig. 5E-H).

#### DGK $\epsilon$ deficiency alters abundance of mitochondrial enzymes

To explore the mechanism for the increase in whole-body lipid oxidation in HFD-fed DGK $\epsilon$  KO mice, we measured key enzymes for mitochondrial abundance and fatty acid metabolism in gastrocnemius muscle. The abundance of citrate synthase (CS), an indicator of mitochondrial

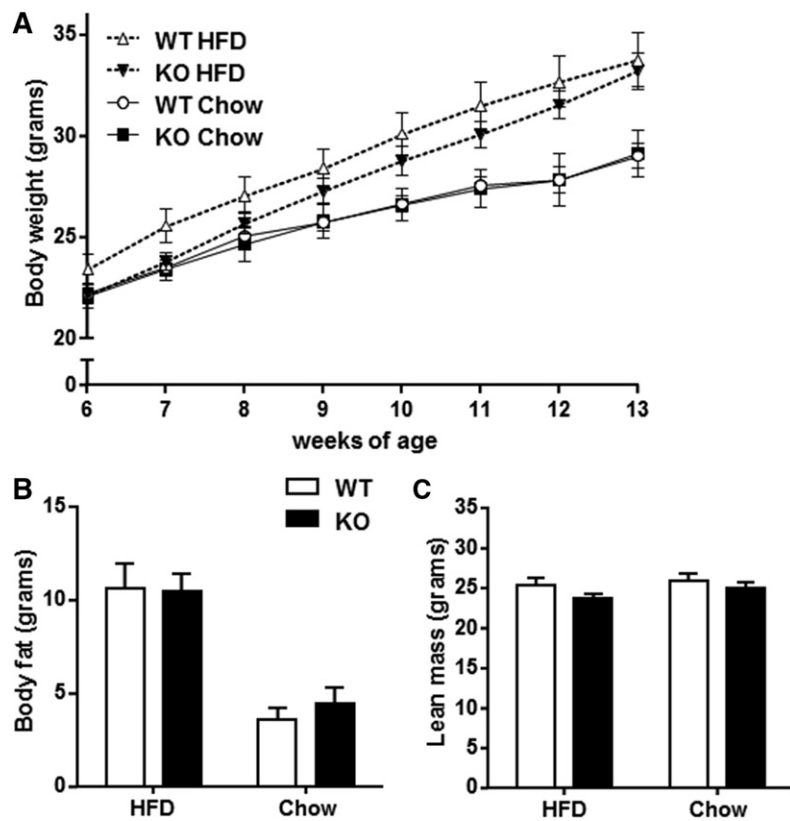


**Fig. 2.** DGK $\epsilon$  is dispensable for growth and maintenance of normal body composition. Body weight of DGK $\epsilon$  KO mice and WT mice fed either HFD or chow was recorded weekly between 6 and 13 weeks of age (A). Total body fat (B) and total lean mass (C) were determined by using EchoMRI. Results are presented as the mean  $\pm$  SEM for HFD-fed WT mice (open triangle/open bar; n = 14–20), HFD-fed DGK $\epsilon$  KO mice (solid triangle/solid bar; n = 11–16), chow-fed WT mice (open circle/open bar; n = 8–10), and chow-fed DGK $\epsilon$  KO mice (solid square/solid bar; n = 7–8).

abundance, was increased in HFD-fed DGK $\epsilon$  KO mice (Fig. 6A). The abundance of 3-hydroxyacyl-CoA dehydrogenase (HADH), an indicator of fatty acid oxidation capacity, tended to increase ( $P = .16$ ) in HFD-fed DGK $\epsilon$  KO mice (Fig. 6B). The abundance of glycerol kinase (GK), a key enzyme in the regulation of glycerol uptake and metabolism, was increased in skeletal muscle from HFD-fed DGK $\epsilon$  KO mice (Fig. 6C).

## DISCUSSION

The phosphorylation and conversion of DAG into PA are catalyzed by a family of DGK isoforms (4, 5). The DGK $\epsilon$  isoform is a ubiquitous membrane-bound enzyme that is constitutively active, with exquisite specificity for DAG species with arachidonic acid in the *sn*-2 position (10, 11). Notably, DGK $\epsilon$  exhibits specificity for DAG species containing the same acyl chain composition found in the phosphatidylinositol cycle (21). Thus, DGK $\epsilon$  has a prominent role in enriching inositol phospholipids with unsaturated fatty acids (12). Because the functional overlap between DGK $\epsilon$  and other DGKs is predicted to be minimal, loss of DGK $\epsilon$  function gives rise to several disease states (15–18, 22). Here we explored the role of DGK $\epsilon$  in the regulation of glucose and energy homeostasis in relation to dietary-induced insulin resistance and obesity. We provide evidence that unsaturated and saturated DAG species are elevated in skeletal muscle of DGK $\epsilon$  KO mice, which is paradoxically associated with increased glucose tolerance. Furthermore, whole-body RER was reduced and mitochondrial marker enzyme levels in skeletal muscle were increased in DGK $\epsilon$

KO mice, indicating increased fat oxidation. Our results suggest that DGK $\epsilon$  influences both glucose and energy homeostasis.

DGK deficiency is predicted to result in an accumulation of DAG species. Several lines of evidence suggest that an accumulation of lipid intermediates in skeletal muscle is associated with insulin resistance (2, 13). We have previously shown that DGK $\delta$  haploinsufficiency results in increased skeletal muscle DAG levels and induces peripheral insulin resistance and mild obesity (7). Moreover, DGK $\delta$  protein abundance is reduced in skeletal muscle from people with type 2 diabetes and regulated by level of glycemia in diabetic animal models (7). However, the role of other DGK isoforms in the development of insulin resistance is unknown. Genetically, obese *ob/ob* mice have reduced DGK $\epsilon$  mRNA expression in skeletal muscle and visceral adipose tissue (19), with profound insulin resistance and impaired lipid metabolism. Consistent with this, here we show that DGK $\epsilon$  ablation increased the level of unsaturated and saturated DAG species in gastrocnemius muscle. However, despite this increase in intramuscular lipids, paradoxically, glucose tolerance, lipid oxidation, and abundance of mitochondrial enzymes were increased in DGK $\epsilon$  KO mice. Our results in DGK $\epsilon$  KO mice indicate that DGK $\epsilon$  deficiency as noted in adipose tissue and skeletal muscle from *ob/ob* mice does not contribute to metabolic disturbances in obesity or type 2 diabetes. Collectively, our results suggest that specific DGK isozymes play specialized roles in the control of glucose and energy homeostasis.

DGK isoforms control the balance of DAG and PA, both of which influence metabolism. Although we were unable to measure PA content in the present study, our model predicts

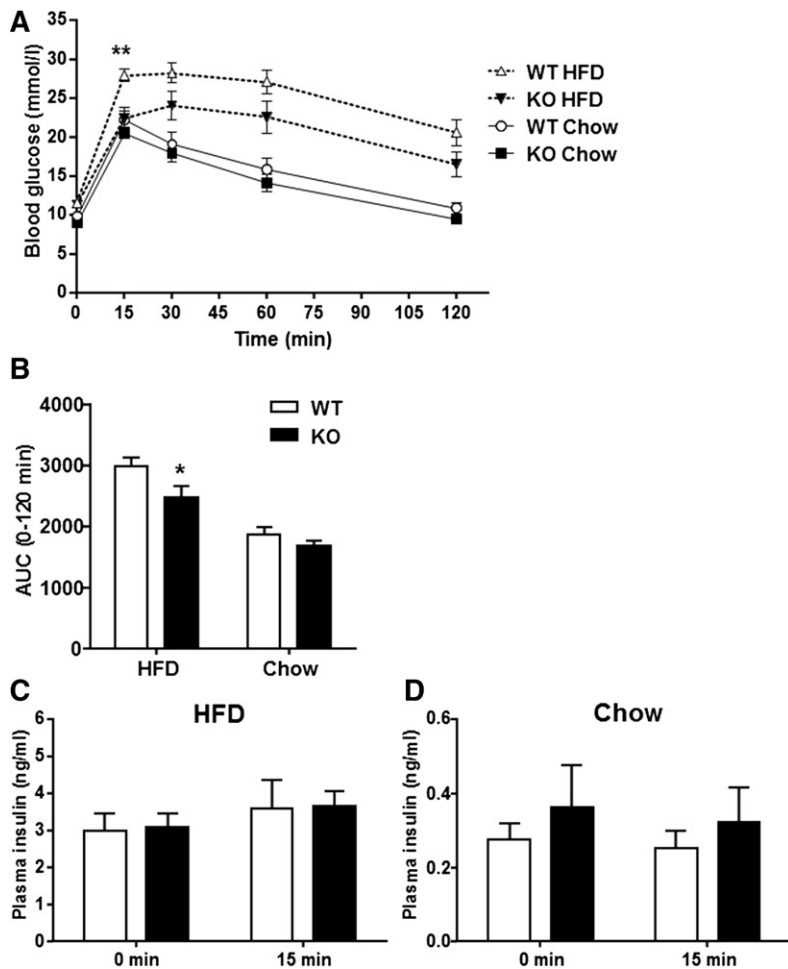


**Fig. 3.** DGK $\epsilon$  deficiency enhances glucose homeostasis. The IPGTT performed in 4 h fasted HFD-fed WT mice (open triangle/open bar;  $n = 14$ ), HFD-fed DGK $\epsilon$  KO mice (solid triangle/solid bar;  $n = 11$ ), chow-fed WT mice (open circle/open bar;  $n = 11$ ), and chow-fed DGK $\epsilon$  KO mice (solid square/solid bar;  $n = 12$ ) (A). AUC for blood glucose in response to the IPGTT (B) in HFD- or chow-fed WT mice and DGK $\epsilon$  KO mice. Plasma insulin before (0 min) and 15 min after the glucose injection in HFD-fed (C) and chow-fed (D) WT mice and DGK $\epsilon$  KO mice. Results are presented as the mean  $\pm$  SEM. \* $P < 0.05$ . \*\* $P < 0.01$  WT versus KO mice on HFD (Student  $t$  test).

that some PA species are likely to be decreased in metabolic tissues because of DGK $\epsilon$  ablation. Thus, effects on glucose and lipid metabolism in DGK $\epsilon$  deficient mice may be mediated by PA-induced signals. For example, PA is a potent activator of atypical protein kinase C (PKC) isoforms (23), and this may be involved in metabolic regulation (24). Increased

atypical PKC activity leads to activation of adenylate cyclase (25), most likely due to the G-protein  $\beta$  subunit phosphorylation (26). As increased adenylate cyclase activity stimulates lipolysis via the cAMP-PKA pathway, lipolysis may be decreased in DGK $\epsilon$  KO mice. Our comprehensive analysis of the skeletal muscle lipidome revealed alterations in several

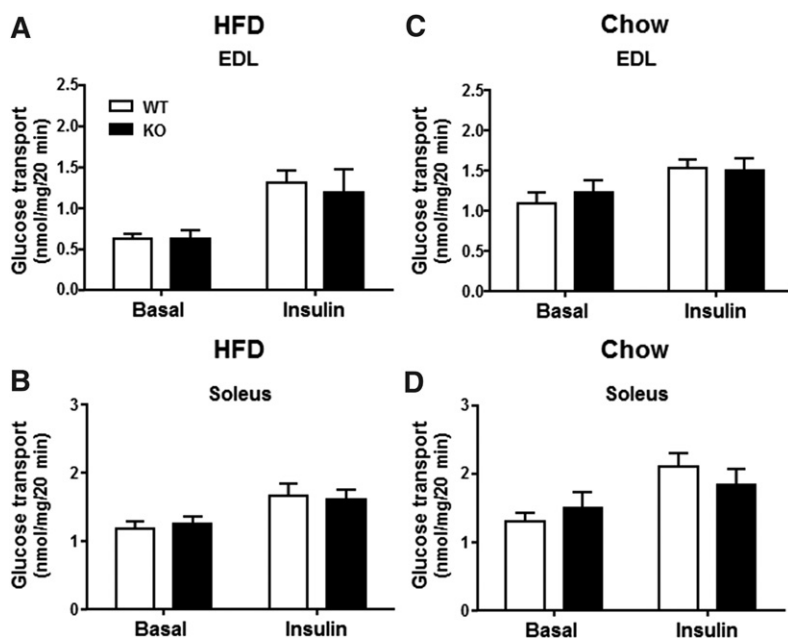


**Fig. 4.** DGK $\epsilon$  deficiency does not alter basal or insulin-stimulated glucose transport in skeletal muscle. Isolated EDL (A, C) and soleus (B, D) muscles were obtained from 4 h fasted HFD- or chow-fed WT mice and DGK $\epsilon$  KO mice and incubated in the absence or presence of a submaximal dose of insulin (0.36 nmol/l) to assess 2-deoxyglucose transport. Results are presented as the mean  $\pm$  SEM for HFD-fed WT mice (open bar;  $n = 18-21$ ) and DGK $\epsilon$  KO mice (solid bar;  $n = 10-12$ ) (A, B) and chow-fed WT mice (open bar;  $n = 7-10$ ) and DGK $\epsilon$  KO mice (solid bar;  $n = 6-7$ ) (C, D).

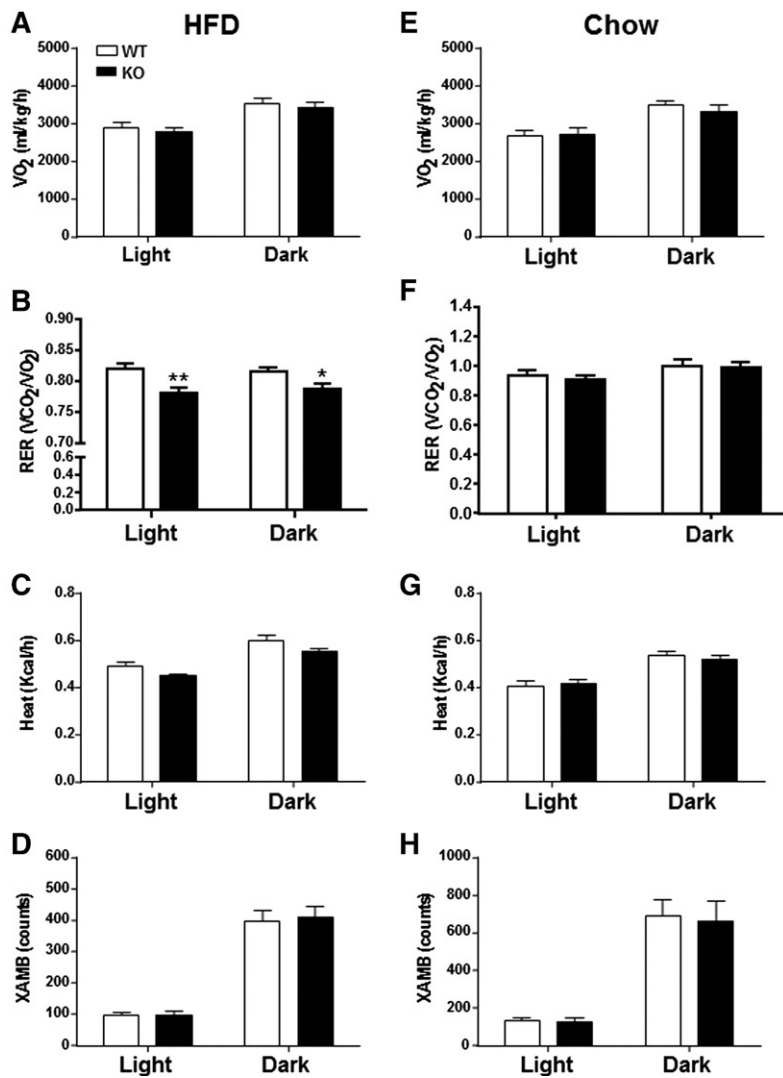


**Fig. 5.** DGK $\epsilon$  deficiency alters energy homeostasis by increasing whole-body lipid oxidation. Oxygen consumption (VO<sub>2</sub>), RER, and energy expenditure (heat) were determined by indirect calorimetry. Spontaneous locomotor activity was recorded. Whole-body energy homeostasis was assessed over 24 h, during the light (sedentary) and dark (active) cycles. VO<sub>2</sub> (A, E), RER (B, F), heat (C, G), and X-AMB (D, H) were determined in HFD- and chow-fed WT mice (open bar; n = 11–13) and DGK $\epsilon$  KO mice (solid bar; n = 10–11). Results are presented as the mean  $\pm$  SEM. \**P* < 0.05. \*\**P* < 0.01 WT versus KO mice on HFD (Student *t* test). X-AMB, X-axis ambulatory activity.

lipid species in DGK $\epsilon$  KO mice. Interestingly, skeletal muscle content of PE tended to increase in DGK $\epsilon$  KO mice (supplemental Table S6), whereas PC content was unaltered (supplemental Table S5). PE content is increased in skeletal muscle from endurance-trained athletes, and PC/PE ratio inversely correlates with insulin sensitivity in humans (27). Thus, a flux of substrates toward *de novo* lipid synthesis may increase free fatty acid (FFA) turnover and therefore increase fatty acid oxidation in DGK $\epsilon$ -deficient mice.

Recent evidence suggests that DGK $\epsilon$  modulates the level of GK (28), an enzyme important for the removal of glycerol produced from lipolysis of triglyceride or diglyceride. In skeletal muscle, low but functional activity of GK is related to the metabolism of fat, which is used to support sustained contractile activity (29). GK is the limiting step in glycerol metabolism in skeletal muscle, and it controls glycerol incorporation into lipids (30). In mouse embryo fibroblasts, DGK $\epsilon$  deficiency leads to increased GK abundance, increased glycerol entrapment in the cell, and consequently, elevated synthesis of glycerol lipids (28). Consistent with this, we found that GK abundance is increased in skeletal muscle from DGK $\epsilon$  KO mice. The increase in GK abundance and glycerol lipid metabolism may provide a

potential mechanism for the increased unsaturated and saturated DAG species in skeletal muscle. Thus, DGK $\epsilon$  affects an early step in lipid synthesis from glycerol, such as glycerol uptake, that affects the synthesis of all lipids.

Strikingly, we found that DGK $\epsilon$  KO mice have reduced RER, indicating a greater reliance on lipid-based fuels. The increase in whole-body lipid oxidation in DGK $\epsilon$  KO mice was further supported by increased abundance of mitochondrial markers in skeletal muscle. Notably, we found that CS, a marker of acyl-CoA mitochondria metabolism (31), was increased in skeletal muscle from DGK $\epsilon$  KO mice. These changes are paradoxical, given the elevated intracellular levels of saturated and unsaturated lipids in skeletal muscle. Our results are consistent with features of the “athlete’s paradox,” in which endurance-trained athletes, who possess a high oxidative capacity and enhanced insulin sensitivity, also have higher intramyocellular lipid content (32, 33). Total DAG content was increased in skeletal muscle from highly insulin-sensitive endurance-trained athletes in comparison with insulin-resistant obese sedentary people (32). The DAG hypothesis for the cause of insulin resistance, though consistent in many models, has been refuted numerous times in other mouse models. For example,



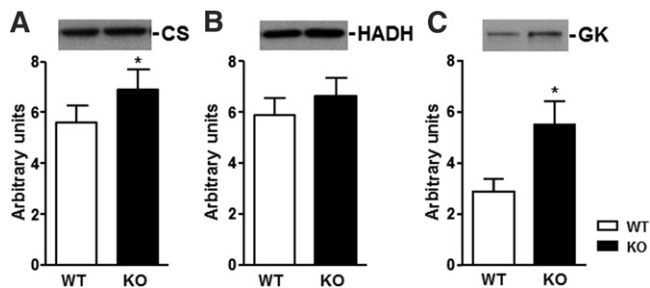


**Fig. 6.** Protein abundance of CS (A), HADH (B), and GK (C) were determined in gastrocnemius muscle from WT (open bar) and DGK $\epsilon$  KO mice (solid bar) on HFD (n = 8). Results are presented as the mean  $\pm$  SEM. \* $P$  < 0.05 versus WT mice (Student  $t$  test).

inhibition of fatty acid oxidation by ethyl-2-[6-(4-chlorophenoxy)hexyl]oxirane-2-carboxylate (etomoxir) results in an accumulation of DAG and TAG in skeletal muscle, with a parallel increase in GLUT4 abundance at the sarcolemma and enhanced glucose homeostasis (34). Additionally, insulin-stimulated glucose uptake postexercise is enhanced in hormone-sensitive lipase KO mice, concomitant with an increase in intramuscular sn-1,3 DAG content (35). Skeletal muscle knockout of CTP-phosphoethanolamine cytidyltransferase leads to DAG accumulation; however, insulin sensitivity is maintained, mitochondrial content, oxidative capacity, and exercise performance are enhanced, and RER is decreased (36). Thus, total cellular DAG content may in some cases be associated with improved insulin sensitivity, challenging the notion that elevated skeletal muscle DAG content leads to insulin resistance.

The cellular localization and stereochemical structure of DAG, rather than the total DAG content, may have a greater influence on skeletal muscle insulin sensitivity (35). Indeed, DAGs may accumulate in different subcellular locations, making them less apt to cause insulin resistance. DGK isoforms alter DAG metabolism in specific cellular compartments because each isoform has a distinct subcellular distribution (4). This may explain why knockdown of DGK $\delta$ , a type II DGK isoform that is predominantly localized intracellularly (4, 37), is associated with insulin resistance (7), whereas knockdown of DGK $\epsilon$ , a type III isoform that is predominantly plasma membrane-bound and constitutively active, protects against insulin resistance. DGK $\delta$  has structural domains that appear to have regulatory roles, including a regulatory pleckstrin homology domain at the amino termini for binding to phosphatidylinositols and sterile  $\alpha$  motif at the C terminus for localization to the endoplasmic reticulum, where it participates in vesicle trafficking (4). The cellular abundance and localization of DGK isoforms, as well as the specific DAG species metabolized, appear to influence insulin sensitivity and energy homeostasis.

The mechanism for the improved glucose tolerance in DGK $\epsilon$  KO mice may be coupled to an increased whole-body lipid oxidation and rapid turnover of intracellular lipids. Paradoxically, both endurance training and high-fat diets are associated with greater reliance on lipid fuel sources for energy. At the molecular level, CS content and activity are

increased in skeletal muscle in response to either exercise training or HFD (38–41). Moreover, protein abundance of HADH in skeletal muscle is increased after exercise training and decreased after deconditioning (42, 43). A systemic signal for these changes may be an increased concentration of circulating plasma lipids or FFAs that target skeletal muscle and induce mitochondria biogenesis, thereby promoting greater fat oxidation (38). Provided lipid oxidation is high, elevated concentrations of lipids stored within muscle fibers may not always lead to insulin resistance. In DGK $\epsilon$  KO mice, the increased intracellular lipids may undergo rapid turnover because of increased mitochondrial function and lipid oxidation, rather than storage, which in turn may preserve insulin sensitivity.

In conclusion, DGK $\epsilon$  plays a role in modulating intracellular lipid metabolism. Lipidomic analysis revealed that DGK $\epsilon$  ablation elevated unsaturated and saturated DAG species in skeletal muscle, which was paradoxically associated with increased glucose tolerance. Although skeletal muscle insulin sensitivity was unaltered in DGK $\epsilon$  KO mice, whole-body RER was reduced, indicating that DGK $\epsilon$  ablation enhances lipid oxidation and preserves insulin sensitivity. Our results support the notion that the capacity for lipid oxidation may be an important determinant in the relationship between excess skeletal muscle lipid accumulation and insulin sensitivity. **FIG**

The authors are grateful to Dr. Matthew K. Topham (University of Utah, Salt Lake City, UT) for providing the DGK $\epsilon$  KO mouse strain.

## REFERENCES

- Erion, D. M., and G. I. Shulman. 2010. Diacylglycerol-mediated insulin resistance. *Nat. Med.* **16**: 400–402.
- Samuel, V. T., and G. I. Shulman. 2012. Mechanisms for insulin resistance: common threads and missing links. *Cell.* **148**: 852–871.
- Wymann, M. P., and R. Schneider. 2008. Lipid signalling in disease. *Nat. Rev. Mol. Cell Biol.* **9**: 162–176.
- Topham, M. K. 2006. Signaling roles of diacylglycerol kinases. *J. Cell. Biochem.* **97**: 474–484.
- Sakane, F., S. Imai, M. Kai, S. Yasuda, and H. Kanoh. 2007. Diacylglycerol kinases: why so many of them? *Biochim. Biophys. Acta.* **1771**: 793–806.
- Sakane, F., S. Imai, M. Kai, I. Wada, and H. Kanoh. 1996. Molecular cloning of a novel diacylglycerol kinase isozyme with a pleckstrin homology domain and a C-terminal tail similar to those of the EPH family of protein-tyrosine kinases. *J. Biol. Chem.* **271**: 8394–8401.
- Chibalin, A. V., Y. Leng, E. Vieira, A. Krook, M. Bjornholm, Y. C. Long, O. Kotova, Z. Zhong, F. Sakane, T. Steiler, et al. 2008. Downregulation of diacylglycerol kinase delta contributes to hyperglycemia-induced insulin resistance. *Cell.* **132**: 375–386.
- Jiang, L. Q., T. de Castro Barbosa, J. Massart, A. S. Deshmukh, L. Lofgren, D. E. Duque-Guimaraes, A. Ozilgen, M. E. Osler, A. V. Chibalin, and J. R. Zierath. 2016. Diacylglycerol kinase-delta regulates ampk signaling, lipid metabolism, and skeletal muscle energetics. *Am. J. Physiol. Endocrinol. Metab.* **310**: E51–E60.
- Decaffmeyer, M., Y. V. Shulga, A. O. Dicu, A. Thomas, R. Truant, M. K. Topham, R. Brasseur, and R. M. Epand. 2008. Determination of the topology of the hydrophobic segment of mammalian diacylglycerol kinase epsilon in a cell membrane and its relationship to predictions from modeling. *J. Mol. Biol.* **383**: 797–809.
- Milne, S. B., P. T. Ivanova, M. D. Armstrong, D. S. Myers, J. Lubarda, Y. V. Shulga, M. K. Topham, H. A. Brown, and R. M. Epand. 2008.



- Dramatic differences in the roles in lipid metabolism of two isoforms of diacylglycerol kinase. *Biochemistry*. **47**: 9372–9379.
11. Shulga, Y. V., M. K. Topham, and R. M. Epand. 2011. Substrate specificity of diacylglycerol kinase-epsilon and the phosphatidylinositol cycle. *FEBS Lett.* **585**: 4025–4028.
  12. Lung, M., Y. V. Shulga, P. T. Ivanova, D. S. Myers, S. B. Milne, H. A. Brown, M. K. Topham, and R. M. Epand. 2009. Diacylglycerol kinase epsilon is selective for both acyl chains of phosphatidic acid or diacylglycerol. *J. Biol. Chem.* **284**: 31062–31073.
  13. Bergman, B. C., D. M. Hunerdosse, A. Kerege, M. C. Playdon, and L. Perreault. 2012. Localisation and composition of skeletal muscle diacylglycerol predicts insulin resistance in humans. *Diabetologia*. **55**: 1140–1150.
  14. Krupp, M., J. U. Marquardt, U. Sahin, P. R. Galle, J. Castle, and A. Teufel. 2012. RNA-seq atlas: a reference database for gene expression profiling in normal tissue by next-generation sequencing. *Bioinformatics*. **28**: 1184–1185.
  15. Rodriguez de Turco, E. B., W. Tang, M. K. Topham, F. Sakane, V. L. Marcheselli, C. Chen, A. Taketomi, S. M. Prescott, and N. G. Bazan. 2001. Diacylglycerol kinase epsilon regulates seizure susceptibility and long-term potentiation through arachidonoyl-inositol lipid signaling. *Proc. Natl. Acad. Sci. USA*. **98**: 4740–4745.
  16. Yamamoto, M., T. Tanaka, Y. Hozumi, S. Saino-Saito, T. Nakano, K. Tajima, T. Kato, and K. Goto. 2014. Expression of mRNAs for the diacylglycerol kinase family in immune cells during an inflammatory reaction. *Biomed. Res.* **35**: 61–68.
  17. Niizeki, T., Y. Takeishi, T. Kitahara, T. Arimoto, M. Ishino, O. Bilim, S. Suzuki, T. Sasaki, O. Nakajima, R. A. Walsh, et al. 2008. Diacylglycerol kinase-epsilon restores cardiac dysfunction under chronic pressure overload: a new specific regulator of G $\alpha$ (q) signaling cascade. *Am. J. Physiol. Heart Circ. Physiol.* **295**: H245–H255.
  18. Lemaire, M., V. Fremeaux-Bacchi, F. Schaefer, M. Choi, W. H. Tang, M. Le Quintrec, F. Fakhouri, S. Taqae, F. Nobili, F. Martinez, et al. 2013. Recessive mutations in dgke cause atypical hemolytic-uremic syndrome. *Nat. Genet.* **45**: 531–536.
  19. Mannerås-Holm, L., H. Kirchner, M. Björnholm, A. V. Chibalin, and J. R. Zierath. 2015. Mrna expression of diacylglycerol kinase isoforms in insulin-sensitive tissues: effects of obesity and insulin resistance. *Physiol. Rep.* **3**: e12372.
  20. Timmers, S., P. Schrauwen, and J. de Vogel. 2008. Muscular diacylglycerol metabolism and insulin resistance. *Physiol. Behav.* **94**: 242–251.
  21. D'Souza, K., and R. M. Epand. 2014. Enrichment of phosphatidylinositols with specific acyl chains. *Biochim. Biophys. Acta*. **1838**: 1501–1508.
  22. Epand, R. M., V. So, W. Jennings, B. Khadka, R. S. Gupta, and M. Lemaire. 2016. Diacylglycerol kinase-epsilon: properties and biological roles. *Front. Cell Dev. Biol.* **4**: 112.
  23. Limatola, C., D. Schaap, W. H. Moolenaar, and W. J. van Blitterswijk. 1994. Phosphatidic acid activation of protein kinase C-zeta overexpressed in cos cells: comparison with other protein kinase c isotypes and other acidic lipids. *Biochem. J.* **304**: 1001–1008.
  24. Farese, R. V., M. C. Lee, and M. P. Sajan. 2014. Atypical pkc: a target for treating insulin-resistant disorders of obesity, the metabolic syndrome and type 2 diabetes mellitus. *Expert Opin. Ther. Targets*. **18**: 1163–1175.
  25. Plesneva, S. A., A. O. Shpakov, L. A. Kuznetsova, and M. N. Pertseva. 2001. A dual role of protein kinase c in insulin signal transduction via adenyl cyclase signaling system in muscle tissues of vertebrates and invertebrates. *Biochem. Pharmacol.* **61**: 1277–1291.
  26. Chakrabarti, S., and A. R. Gintzler. 2003. Phosphorylation of gbeta is augmented by chronic morphine and enhances gbetagamma stimulation of adenyl cyclase activity. *Brain Res. Mol. Brain Res.* **119**: 144–151.
  27. Newsom, S. A., J. T. Brozinick, K. Kiseljak-Vassiliades, A. N. Strauss, S. D. Bacon, A. A. Kerege, H. H. Bui, P. Sanders, P. Siddall, T. Wei, et al. 2016. Skeletal muscle phosphatidylcholine and phosphatidylethanolamine are related to insulin sensitivity and respond to acute exercise in humans. *J. Appl. Physiol.* **120**: 1355–1363.
  28. So, V., D. Jalan, M. Lemaire, M. K. Topham, G. M. Hatch, and R. M. Epand. 2016. Diacylglycerol kinase epsilon suppresses expression of p53 and glycerol kinase in mouse embryo fibroblasts. *Biochim. Biophys. Acta*. **1861**: 1993–1999.
  29. Newsholme, E. A., and K. Taylor. 1969. Glycerol kinase activities in muscles from vertebrates and invertebrates. *Biochem. J.* **112**: 465–474.
  30. Montell, E., C. Lerin, C. B. Newgard, and A. M. Gómez-Foix. 2002. Effects of modulation of glycerol kinase expression on lipid and carbohydrate metabolism in human muscle cells. *J. Biol. Chem.* **277**: 2682–2686.
  31. Kastaniotis, A. J., K. J. Autio, J. M. Keratar, G. Monteuuis, A. M. Makela, R. R. Nair, L. P. Pietikainen, A. Shvetsova, Z. Chen, and J. K. Hiltunen. 2017. Mitochondrial fatty acid synthesis, fatty acids and mitochondrial physiology. *Biochim. Biophys. Acta*. **1862**: 39–48.
  32. Amati, F., J. J. Dube, E. Alvarez-Carnero, M. M. Edreira, P. Chomentowski, P. M. Coen, G. E. Switzer, P. E. Bickel, M. Stefanovic-Racic, F. G. Toledo, et al. 2011. Skeletal muscle triglycerides, diacylglycerols, and ceramides in insulin resistance: another paradox in endurance-trained athletes? *Diabetes*. **60**: 2588–2597.
  33. Goodpaster, B. H., J. He, S. Watkins, and D. E. Kelley. 2001. Skeletal muscle lipid content and insulin resistance: evidence for a paradox in endurance-trained athletes. *J. Clin. Endocrinol. Metab.* **86**: 5755–5761.
  34. Timmers, S., M. Nabben, M. Bosma, B. van Bree, E. Lenaers, D. van Beurden, G. Schaart, M. S. Westerterp-Plantenga, W. Langhans, M. K. Hesselink, et al. 2012. Augmenting muscle diacylglycerol and triacylglycerol content by blocking fatty acid oxidation does not impede insulin sensitivity. *Proc. Natl. Acad. Sci. USA*. **109**: 11711–11716.
  35. Serup, A. K., T. J. Alsted, A. B. Jordy, P. Schjerling, C. Holm, and B. Kiens. 2016. Partial disruption of lipolysis increases postexercise insulin sensitivity in skeletal muscle despite accumulation of dag. *Diabetes*. **65**: 2932–2942.
  36. Selathurai, A., G. M. Kowalski, M. L. Burch, P. Sepulveda, S. Risis, R. S. Lee-Young, S. Lamou, P. J. Meikle, A. J. Genders, S. L. McGee, et al. 2015. The CDP-ethanolamine pathway regulates skeletal muscle diacylglycerol content and mitochondrial biogenesis without altering insulin sensitivity. *Cell Metab.* **21**: 718–730.
  37. Miele, C., F. Paturzo, R. Teperino, F. Sakane, F. Fiory, F. Oriente, P. Ungaro, R. Valentino, F. Beguinot, and P. Formisano. 2007. Glucose regulates diacylglycerol intracellular levels and protein kinase C activity by modulating diacylglycerol kinase subcellular localization. *J. Biol. Chem.* **282**: 31835–31843.
  38. Garcia-Roves, P., J. M. Huss, D. H. Han, C. R. Hancock, E. Iglesias-Gutierrez, M. Chen, and J. O. Holloszy. 2007. Raising plasma fatty acid concentration induces increased biogenesis of mitochondria in skeletal muscle. *Proc. Natl. Acad. Sci. USA*. **104**: 10709–10713.
  39. Reichmann, H., R. Wasl, J. A. Simoneau, and D. Pette. 1991. Enzyme activities of fatty acid oxidation and the respiratory chain in chronically stimulated fast-twitch muscle of the rabbit. *Pflugers Arch.* **418**: 572–574.
  40. Galuska, D., O. Kotova, R. Barres, D. Chibalina, B. Benziane, and A. V. Chibalin. 2009. Altered expression and insulin-induced trafficking of Na<sup>+</sup>-K<sup>+</sup>-ATPase in rat skeletal muscle: effects of high-fat diet and exercise. *Am. J. Physiol. Endocrinol. Metab.* **297**: E38–E49.
  41. Hancock, C. R., D. H. Han, M. Chen, S. Terada, T. Yasuda, D. C. Wright, and J. O. Holloszy. 2008. High-fat diets cause insulin resistance despite an increase in muscle mitochondria. *Proc. Natl. Acad. Sci. USA*. **105**: 7815–7820.
  42. Lammers, G., F. Poelkens, N. T. van Duijnhoven, E. M. Pardoel, J. G. Hoenderop, D. H. Thijssen, and M. T. Hopman. 2012. Expression of genes involved in fatty acid transport and insulin signaling is altered by physical inactivity and exercise training in human skeletal muscle. *Am. J. Physiol. Endocrinol. Metab.* **303**: E1245–E1251.
  43. Tunstall, R. J., K. A. Mehan, G. D. Wadley, G. R. Collier, A. Bonen, M. Hargreaves, and D. Cameron-Smith. 2002. Exercise training increases lipid metabolism gene expression in human skeletal muscle. *Am. J. Physiol. Endocrinol. Metab.* **283**: E66–E72.